

PAPER • OPEN ACCESS

## Investigation of water column separation induced by pressure pulsation based on critical cavitation rate model

To cite this article: J B Yang *et al* 2021 *IOP Conf. Ser.: Earth Environ. Sci.* **774** 012055

View the [article online](#) for updates and enhancements.

You may also like

- [Physical model studies of water column separation](#)  
R Autrique, E Rodal, A Sánchez et al.
- [Testing the Retrieval of Inner Disk Water Enrichment with Spitzer/IRS and JWST/MIRI](#)  
Mackenzie M. James, Ilaria Pascucci, Yao Liu et al.
- [Study on Judgment and calculation method of two water column separation water hammer](#)  
Li Zhao, Yusi Yang, Tong Wang et al.



**ECS**  
The  
Electrochemical  
Society  
Advancing solid state &  
electrochemical science & technology

**DISCOVER**  
how sustainability  
intersects with  
electrochemistry & solid  
state science research

# Investigation of water column separation induced by pressure pulsation based on critical cavitation rate model

J B Yang<sup>1,2</sup>, J D Yang<sup>2</sup>, W C Guo<sup>3</sup>, J J Luo<sup>1</sup>, G F Fu<sup>1</sup>

<sup>1</sup> Zhongnan Engineering Corporation Limited, Power Construction Corporation China, Changsha, 410014, China

<sup>2</sup> State Key Laboratory of Water Resources and Hydropower Engineering Science, Wuhan University, Wuhan, 430072, China

<sup>3</sup> School of Hydropower and Information Engineering, Huazhong University of Science and Technology, Wuhan, 430074, China

Corresponding author: W C Guo, E-mail: wencheng@hust.edu.cn

**Abstract:** Significant pressure fluctuation may exist at the inlet of the draft pipe during load shedding of water pump and turbine sets. When the tail-water level is low, the minimum water hammer pressure at the inlet of the draft pipe set is higher than evaporation pressure; however, the overall pressure after superposition with pulsating pressure may reach the evaporation pressure in an instant. In these cases, it is unknown if a cavity is formed or water column separation is induced. It is also unknown how frequency and amplitude of the pulsating pressure affect the formation of cavity or water column separation. However, in terms of the physical formation of water column separation, liquid pressure reaching evaporation pressure is only the necessary condition of water column separation rather than a sufficient condition because the growth and aggregation of cavitations take time. In addition, water column separation could be induced only when the cavitation rate in the water reaches a specific value and gas-liquid relative motion occurs. In this study, based on the uniform cavitation distribution model, the critical of flow velocity gradients are calculated both in front and at the back of the section and are the sufficient condition of water column separation. This study uses the criterion of when the ratio of the vaporous cavitation volume to the volume of the pipe segment with a length of  $\Delta x$  exceeds a critical cavitation rate for classifying water column separation segments and non-water column separation segments. In water column separation segments, a concentrated vaporous cavitation model is used for calculation; however, dynamic meshes should be applied for tracking the change of vaporous cavitations. In the non-water column separation segments, the vaporous cavitation volume can be calculated according to the continuity equation but is converted into a cavitation rate in the pipe segment and substituted into gas-liquid two-phase equation to calculate wave velocity. Next, a case study was performed on a pipe-valve system. By taking into account the pulsating pressures with different frequencies and amplitudes on the downstream side in the valve closing process, water column separation and merging processes were analyzed and the change in flows, cavitation volumes and pressures on various sections and their laws during the transient process were concluded.

## 1. Introduction

There tends to exist significant pressure fluctuation at the inlet of the draft pipe during load shedding of the water pump and turbine sets. At a low level of tailwater, although the minimum water hammer pressure at the inlet of the unit draft pipe is higher than the evaporation pressure, the overall pressure after the superposition of pulsating pressures may reach the evaporation pressure in an instant.



Under that condition, cavities or water column separation may be formed. It is unknown exactly how the pulsation pressure frequency and amplitude affect the formation of cavities and the separation of water column. However, in terms of the physical process of water column separation, when the pressure intensity approaches or drops to the evaporation pressure intensity. The dissolved gas nuclei in the fluid expand rapidly and bond with the neighboring gas nuclei, forming vaporous cavitations. The small cavitations then expand, and some vaporous cavitations form after reaching the critical stability radius. When rising to the pipe top, the vaporous cavitations continue to grow along the pipe and bond to form large immobile cavitations. At the inflection point of the pipe or the high point (i.e., the critical point), large cavitations may result in the separation of water column at the cross-section with a high flow velocity gradient. In other words, the decrease of liquid pressure to the evaporation pressure is the only necessary condition rather than being a sufficient condition for water column separation. Only when the cavitation rate in water reaches a specific value and liquid-gas motion occurs can water column separation be induced.

Based on the existing uniform cavitation distribution model [1-5], this study adopted the critical value of the flow velocity gradient before and after the section as the necessary condition of water column separation. A pipe segment with a length of  $\Delta x$  can be divided into the water column separation segment and non-water column separation segment according to the criterion whether the ratio of the volume of the vaporous cavitations to the volume of the pipe segment exceeds the critical cavitation rate. In the water column separation segment, the concentrated vaporous cavitation model can be used for calculation; however, dynamic meshes should be generated for tracking the change in the volume of vaporous cavitations. In the non-water column separation segment, the volume of the vaporous cavitation can also be calculated according to the equation of continuity. However, the volume of vaporous cavitation can be converted into the cavitation rate in this segment and substituted into the gas-liquid two-phase equation to calculate the other parameters such as wave velocity. Next, using the model, the pipe-valve system was calculated, i.e., the pulsating pressures with different frequencies, amplitudes, phases, and attenuation values were included during the valve closing process to analyze the water column separation and bridging evolution process. Moreover, variations in the flow rate, cavitation volume and pressure at different sections during the transient process as well as their controls were concluded.

## 2. Mathematical model

### 2.1. Uniform cavitation distribution model

The flow accompanied by gas release and water column separation can be divided into three regions using the uniform cavitation distribution model — conventional water hammer region, cavitation region, and water column separation region. In the cavitation region, the fluid flow pattern can be approximately regarded as vesicular gas-liquid two-phase flow and countless small cavitations are uniformly mixed and flow with the liquid. In the water column separation region, gas release in the water column separation and the phase change effect in the evaporation of liquid are considered. Simultaneously, the effect of gas content in the cavitation flow near the water column separation position on the wave velocity of water hammer is also taken into account. Overall, this model is a combination of gas-containing gas-liquid two-phase flow and the vaporous cavitation model. During the transient process, different flow regions, namely, gas-containing cavitation flow without gas release (i.e., when the pressure of gas/liquid mixed fluid  $p$  is higher than gas saturated pressure  $p_s$ ), gas-containing cavitation flow with gas release (i.e., when the pressure of gas/liquid mixed fluid is less than gas saturated pressure  $p_s$ ), and vaporous cavitation (water column separation) may all appear in the cavitation pipe.

#### 2.1.1. Model of transient flow equation of gas-containing cavitation flow without gas release

The basic equation of gas-liquid two-phase transient flow includes the momentum equation and continuity equation for gas-phase and liquid-phase. Because the cavitations in gas-containing

gas-liquid two-phase transient flow have a small volume and move together with the liquid, the momentum exchange between the two phases are ignored. Therefore, the momentum equations can be combined into one equation, while the two continuity equations for the gas and liquid remain unchanged to take into account the mass transfer between two phases.

(1) Momentum equation

$$\frac{\partial V}{\partial t} + V \frac{\partial V}{\partial x} + \frac{1}{\rho_m} \frac{\partial p}{\partial x} + g \sin \theta + \frac{f}{2D} V |V| = 0 \quad (1)$$

where  $x$  denotes the coordinate distance along the pipe axis from any a starting point, with a unit of m;  $\theta$  denotes the included angle between the connecting line of the centroids of various sections and the horizontal plane (with a positive downslope);  $p$  denotes the pressure at the pipe center point, with a unit of m;  $v$  denotes the flow velocity at the section, with a unit of m<sup>3</sup>/s;  $D$  denotes the diameter of the pipe, with a unit of m;  $\rho$  denotes the density of gas-liquid two-phase mixed fluid, with a unit of kg/m<sup>3</sup>;  $\alpha$  denotes the cavitation rate;  $f$  denotes the friction loss efficient.

(2) Continuity equation

The mass exchange rate between phases can be denoted as  $\dot{m} = dm/dt$ . According to the law of conservation of mass, the following equations are derived:

$$\text{For gas phase: } \frac{\partial}{\partial t}(\rho_g \alpha A) + \frac{\partial}{\partial x}(\rho_g \alpha AV) = \dot{m}A \quad (2)$$

$$\text{For liquid phase: } \frac{\partial}{\partial t}[\rho_l(1-\alpha)A] + \frac{\partial}{\partial x}[\rho_l(1-\alpha)AV] = -\dot{m}A \quad (3)$$

where  $A$  denotes the sectional area, and the subscripts  $g$  and  $l$  represent gas phase and liquid phase, respectively. By summing Equation 2 and Equation 3, the following expression can be derived:

$$\frac{\partial}{\partial t}(\rho_m A) + \frac{\partial}{\partial x}(\rho_m AV) = 0 \quad (4)$$

Equation 2 and Equation 3 constitute a two-equation mathematical model of gas-containing gas-liquid two-phase transient flow. The partial differential equation can be transformed using the characteristic line method into the following ordinary differential equations of two clusters along the characteristic line:

$$C^+ : \begin{cases} \frac{1}{\rho_m a} \frac{dp_m}{dt} + \frac{dV}{dt} + g \sin \theta + \frac{f}{2D} V |V| = 0 \\ \frac{dx}{dt} = V + a \end{cases} \quad (5)$$

$$C^- : \begin{cases} -\frac{1}{\rho_m a} \frac{dp_m}{dt} + \frac{dV}{dt} + g \sin \theta + \frac{f}{2D} V |V| = 0 \\ \frac{dx}{dt} = V - a \end{cases} \quad (6)$$

When  $p_m > p_s = 76000\text{Pa}$ , gas release is not taken into account. Without the appearance of liquid column separation, the following equations should be introduced:

$$\alpha = \frac{\frac{4}{3} \pi R^3 N_b}{A \Delta x} \quad (7)$$

$$p_m = (p_g + p_v) \alpha + p_l (1 - \alpha) \quad (8)$$

$$p_l = p_g + p_v - \frac{2\sigma}{R} \quad (9)$$

$$p_g \left( \frac{4}{3} \pi R^3 N_b \right) = p_{g0} \left( \frac{4}{3} \pi R_0^3 N_b \right) = m_{g0} \frac{K}{M} T \quad (10)$$

$$\rho_m = \rho_g \alpha + \rho_l (1 - \alpha) \quad (11)$$

$$\rho_g = \frac{m_{g0}}{W_g} = \frac{m_{g0}}{\frac{4}{3}\pi R^3 N_b} \quad (12)$$

$$\alpha^2 = \frac{\frac{K_l}{\rho_m}}{\frac{\frac{\rho_l + \alpha\rho_l}{\rho_m} \left( \frac{3K_l}{3rp_g - 2\sigma/R} - 1 \right)}{1 - \frac{4\alpha\sigma/R}{\left( 3rp_g - \frac{2\sigma}{R} \right)}} + \frac{K_l DC_1}{Ee}} \quad (13)$$

where  $p_m$  denotes the pressure of gas-liquid mixed fluid,  $p_g$  denotes the pressure of gas-phase,  $p_l$  denotes the pressure of liquid-phase,  $\rho_m$  denotes the density of gas-liquid mixed fluid,  $\rho_g$  denotes the gas-phase density,  $R$  denotes the cavitation diameter,  $\alpha$  denotes the cavitation rate,  $a$  denotes the wave velocity and  $V$  denotes the flow velocity. Eqs. (5)~(13) constitute the mathematical model of the gas-containing cavity flow without the appearance of liquid column separation when gas release is not taken into account.

The other parameters can be defined as.  $N_b$  denotes the number of cavitations in the pipe segment per unit volume with a length of  $\Delta x$  and an area of  $A$ ,  $p_v$  denotes the evaporation pressure,  $\sigma$  denotes the surface tension coefficient,  $\alpha_0$  denotes the initial cavitation rate,  $W_{g0}$  denotes the sum of the initial cavitation volume,  $R_0$  denotes the initial cavitation radius,  $p_{g0}$  denotes the initial gas pressure,  $K$  denotes gas constant,  $T$  denotes Kelvin temperature,  $M$  denotes the air's molar mass,  $m_{g0}$  denotes initial air mass,  $\rho_{g0}$  denotes the initial air density,  $K_l$  denotes the elasticity modulus of liquid (water),  $C_1$  denotes the supporting mode of pipe,  $E$  denotes the elasticity modulus of the pipe wall, and  $e$  denotes the wall thickness.

During the solving process, Equation 5 and Equation 6 are first converted to the algebraic equations Equation 14 and Equation 15, and  $p_{mP}$  and  $V_p$  can be solved by means of interpolation in characteristic line network.

$$V_p = Q_{CP} - C_{QP} p_{mP} \quad (14)$$

$$V_p = Q_{CM} + C_{QM} p_{mP} \quad (15)$$

in which

$$C_{QP} = \left( \frac{1}{\rho_m a} \right)_R, \quad Q_{CP} = \left[ \left( \frac{1}{\rho_m a} \right)_R p_{mR} + V_R - \left( g \sin \theta + \frac{f}{2D} V_R |V_R| \right) (t_P - t_R) \right]$$

$$C_{QM} = \left( \frac{1}{\rho_m a} \right)_S, \quad Q_{CM} = \left[ - \left( \frac{1}{\rho_m a} \right)_S p_{mS} + V_S - \left( g \sin \theta + \frac{f}{2D} V_S |V_S| \right) (t_P - t_S) \right]$$

The other gas parameters can be solved using Eqs. (7)~(13).

### 2.1.2. Mathematical model of the transient-flow equation of gas-containing cavitation with gas release

By taking into account surface tension, gas release rate can be calculated as:

$$\frac{dm_g}{dt} = 4\pi R D \beta (p_s - p_g) \left\{ 1 - \frac{2\sigma}{3Rp_g} \right\} \quad (16)$$

where  $D$  denotes the diffusion coefficient,  $\beta$  denotes Henry's constant, with a unit of mol/J,  $p_s$  denotes the saturation pressure;  $R$  denotes the cavitation radius;  $p_g$  denotes the pressure of gas-phase.

When  $p_m < p_s = 76000\text{Pa}$ , gas release should be considered, and Equation 10 and Equation 12 should be revised as:

$$p_g \left( \frac{4}{3} \pi R^3 N_b \right) = m_g \frac{K}{M} T \quad (17)$$

$$\rho_g = \frac{m_g}{W_g} \quad (18)$$

The following Equation 19 is also added:

$$m_g = m_{g0} + 4\pi R D \beta (p_s - p_g) \left\{ 1 - \frac{2\sigma}{3R p_g} \right\} \Delta t \quad (19)$$

Equations 5, 6, 7, 8, 9, 11, 13, 17, 18 and 19 constitute the gas-containing cavity flow transient equation with the consideration of gas release. During the solving process,  $p_{mP}$  and  $V_p$  are first solved using Equation 14 and Equation 15, and the other gas parameters are solved according to the other gas parameter equations.

### 2.1.3. Mathematical model of vapor-containing cavity flow and liquid column separation

According to the physical process of the initiation, expansion or shrinkage and collapse of vaporous cavitations, the mathematical model can be established below: If the initial volume of vaporous cavity equals to 0, i.e.,  $\forall_{cav0} = 0$ , when  $p_{mP} \leq p_v$ , let  $p_{mP} = p_v$ .

$$V_{Pu} = Q_{CP} - C_{QP} p_v \quad (20)$$

$$V_{Pd} = Q_{CM} + C_{QM} p_v \quad (21)$$

$$\forall_{cav} = \forall_{cav0} + A(V_{Pd} - V_{Pu}) \Delta t \quad (22)$$

By combining Eqs. (20)~(22),  $V_{Pu}$ ,  $V_{Pd}$  and  $\forall_{cav}$  can be solved. If  $\forall_{cav} \leq 0$ , let  $\forall_{cav} = 0$ ,  $V_{Pu} = V_{Pd} = V_p$ ,  $p_{mP}$  and  $V_p$  can be solved by combining Equation 14 and Equation 15.

### 2.2. Uniform cavitation distribution model based on critical cavitation rate

According to the description in Section 2.1.1 and Section 2.1.2, when the pressure of the gas-liquid mixed fluid exceeds the saturation pressure of the gas (i.e.,  $p_{mP} > p_s$ ), the gas-containing cavitation flow model without gas release should be used for calculations; when  $p_{mP} \leq p_s$ , the gas-containing cavity flow model with gas release should be used for calculations.

When the pressure at the node j is below the evaporation pressure, it can be set as  $p_{mP} = p_v$ . The volume of the vaporous cavitation is then calculated according to Equation 22, and meanwhile, the cavity rate  $\alpha$  can be calculated as:

$$\alpha = \frac{\forall_{cav} + \forall_g}{A \Delta x} \quad (23)$$

When  $\alpha$  is below the critical cavitation rate  $\alpha_c$ , the vaporous cavitation can move together with liquid and no liquid column separation occurs. Let  $v = \frac{1}{2}(V_{Pu} + V_{Pd})$ , the condition at the next moment is calculated. When  $\alpha$  exceeds  $\alpha_c$ , the vaporous cavitation at the node cannot move with liquid and water column separation appears. The volume of the great cavitation that blocks the flow can be written as:  $\forall'_{cav} = \forall'_{cav0} + A(V_{Pd} - V_{Pu}) \Delta t$ .

If  $\forall'_{cav} > 0$  and  $\alpha > \alpha_c$ , water column separation still exists. The condition at the next moment still follows water column separation model and the cavitation rate  $\alpha$  is calculated. If  $\forall'_{cav} < 0$ , large cavitations for blocking water flow have been merged; however, at that moment,  $p_{mP} = p_v$ . The change in the volume of small cavitation can also be calculated according to Equation 23, in which

$V = \frac{1}{2}(V_{pu} + V_{pd})$ . Small cavitation is considered to flow with water. When  $\nabla_{cav} = 0$ , small cavitations are finally ruptured and collapse, and the condition is calculated according to gas-containing cavity flow model.

### 2.3. Superposition with pulsating pressure

By taking the pulsating pressure into account, the uniform cavitation distribution model with consideration of the critical cavitation rate can be solved according to the following procedures.

Step 1 Pulsating pressure is not considered in the momentum equation, and the continuity equation of gas-liquid two-phase transient flow, (i.e.,  $p_{mP}$  in Eq (5) and Eq (6)) still denotes the water hammer pressure of the gas-liquid mixed fluid pressure.  $p_{mP}$  and  $V_P$  are still solved according to Equation 14 and Equation 15.

Step 2 The overall pressure equals to the superposition of the calculated  $p_{mP}$  and the pulsating pressure  $p'_{mP}$ , i.e.,  $p_{mZ} = p_{mP} + p'_{mP}$ . Whether the overall pressure reaches the gas saturation pressure  $p_s$  is regarded as the criterion of gas release, while whether  $p_{mZ}$  reaches the evaporation pressure  $p_v$  is regarded as the criterion of the formation of vaporous cavitation.  $p_{mP}$  is replaced by the superposed pressure, i.e., the overall pressure  $p_{mZ}$ , in solving the cavitation radius  $R$ , the cavitation rate  $\alpha$ , the cavitation volume  $W_g$ , the gas density  $\rho_g$ , the mixture density  $\rho_m$  and the wave velocity of mixture  $a$ .

It should be noted that when the calculated  $p_{mP}$  according to characteristic line equation  $p_{mP}$  or the superposed pressure  $p_{mZ}$  is below the evaporation pressure  $p_v$ , let  $p_{mP}$  or  $p_{mZ}$  equal to  $p_v$  since they cannot be below the evaporation n pressure.

### 3. Case study

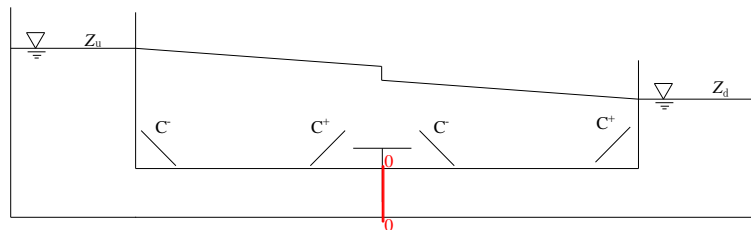


**Figure 1.** Illustration of water piping system.

Figure 1 displays a horizontal water delivery piping system including the upper reservoir, the valve and the lower reservoir, in which the center line of the pipe is set as the datum line. The water level of the upper reservoir exceeds the pipe center line by 10.0 m and the water level of the lower reservoir is 5.2181 m higher than the pipe center line. A valve is set in the middle of the pipe. The pipe segments in front of and at back of the valve are all 40 m in length and 0.5 m in diameter. The numbers of pipe segments in front of and at back of the valve are both 20 ( $N=20$ ), i.e.,  $\Delta x = 2\text{m}$ . The pipe roughness  $n$  is set as 0.012(-). The other parameters related to air in the pipe segment are set below. The number of the cavitations in the pipe segment per unit volume with a length of and an area of  $A$ , denoted as  $N_b$ , was set as  $10^6$ . The evaporation pressure ( $p_v$ ) and the surface tension coefficient ( $\sigma$ ) were set as 2430 Pa and  $7.28 \times 10^{-2} \text{N/m}$ , respectively. The initial cavitation rate ( $\alpha_0$ ), the initial air mass and the initial air density were set as  $10^{-5}$ ,

$m_{g0} = p_{g0} \left( \frac{4}{3} \pi R_0^3 N_b \right) \frac{T}{K}$  and  $\rho_{g0} = \frac{m_{g0} M}{W_{g0} * 1000}$ , respectively. The air molar mass ( $M$ ) and air molar volume

were set as 29 g/mol and 22.4 L/mol, respectively. The elasticity modulus of liquid (water), denoted as  $K_l$ , was set as  $20.6 \times 10^8 \text{ N/m}^2$ . The pipe supporting mode ( $C_1$ ) was set as 1. The elasticity modulus and the thickness of the pipe wall, denoted as  $E$  and  $e$ , were set as  $206 \times 10^9 \text{ N/m}^2$  and 0.03 m, respectively.

### 3.1. Calculation results after taking into account true pulsating pressure

As shown in Figure 2, the valve 3.0 s was linearly closed so that the water hammer pressure at the 0-0 section on the downstream side of the valve was nearly 0 m (i.e., the absolute pressure). Next, pulsating pressures with identical frequencies and amplitudes to these at the inlet of No. 4# tailpipes during a test in the Heimifeng Pumped Storage Power Station were applied. Figure 3 also shows the pulsating pressure on the 0-0 Section. Letting the pulsating pressure on various sections on the upstream side of the valve decrease progressively according to Equation 24 (i.e., the square root of the reciprocal to the distance from the 0-0 Section), the changes in the pressure and cavity volume on the downstream side of the valve were analyzed to determine if water column separation can be induced.

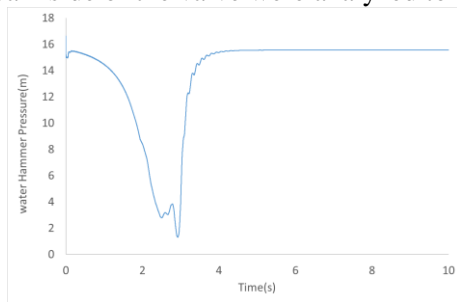


**Figure 2.** Closing rule of the valve.

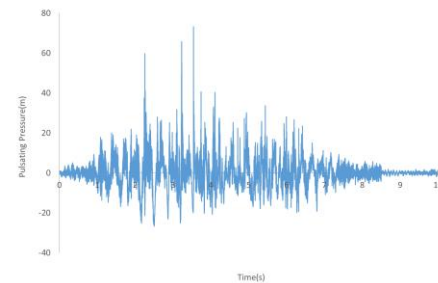


**Figure 3.** Pulsating pressure on the 0-0 section.

$$p'_{mP}(x_n) = p'_{mP}(0)(x_n - x_0)^{-1/2} \quad (24)$$

The maximum downward pulsating pressure appeared at approximately 2.5s and reached up to -27.00m. The pulsating pressure on the 0-0 Section at different periods (2~3s and 5~6s), as shown in Figure 4, demonstrate that the pulsation was composed of the superposition of a low-frequency fundamental wave and a high-frequency carrier wave. As shown in Figure 4, three obviously negative low-frequency fluctuations occurred in the periods 2.1~2.2s, 2.45~2.55s, and 2.82~2.89s, respectively, with a period of approximately 0.2s (or negative-pressure lasting approximately 0.1s) and an amplitude of over -20.0m. After local time amplifying, the fluctuation period of the high-frequency wave was approximately 0.004s and a downward amplitude was at its maximum at 2.25s and exceeded -20.0m. It can be observed from Figure 4 that the downward amplitude did not exceed 20.0 m within 5~6s on the 0-0 Section. The fluctuation period of the low-frequency wave lasted for less than 0.1s (or negative pressure lasted approximately 0.05s) and the fluctuation period of the high-frequency wave was approximately 0.007s.

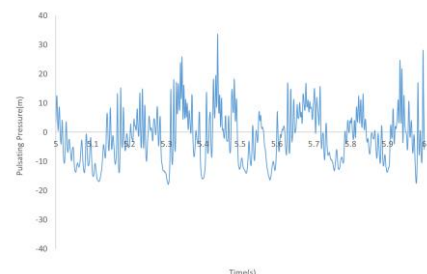
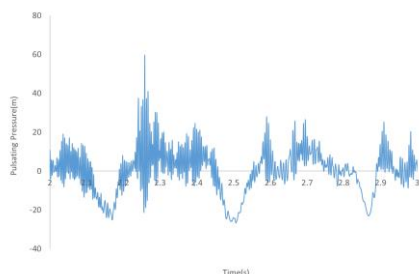


**Figure 4.** Pulsating pressure on the 0-0 Section with in 2~3s and 5~6s.

By setting the critical cavitation rate as 0.05, 0.10 and 0.15, respectively, the changes of the volume of cavitation volumes in the segment between the 0-0 Section and the 1-1 Section when the overall pressure reaches the evaporation pressure and liquid column separation occurs and the pressure on the 0-0 Section were analyzed, as shown in Figure 5~Figure 7. The pressure curve of the 0-0 Section

reached the evaporation pressure three times within 2~3 s. The time slots were close to continuous low-frequency negative pressure time as shown in Figure 4. Water column separation occurred from 0-0 Section to 1-1 Section at approximately 2.9s. At a critical cavitation rate of 0.05, water column separation occurred from 0-0 Section to 1-1 Section within 5~6s. At a critical cavitation rate of 0.10 and 0.15, in spite of the occurrence of vaporous cavitation, the condition of water column separation was not satisfied. After the collapsing of water columns, as shown in Figs. 2.7~2.9, the pressures of 0-0 Section within 2~3 s at three critical cavitation rates reached up to 265.0m, 427.0m and 416.0m, respectively. At a critical cavitation rate of 0.05, the calculated pressure of the 0-0 Section within 5~6s reached up to 409m, which were 229.0m and 74.0m at a critical cavitation rate of 0.1 and 0.15, respectively.

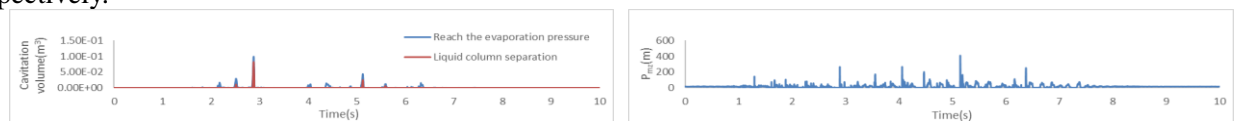


**Figure 5.** Cavitation volumes and pressure changes at a critical cavitation rate of 0.05.

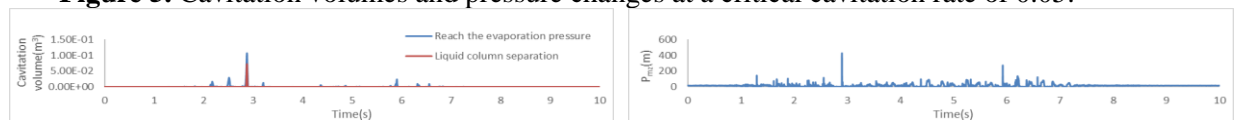


**Figure 6.** Cavitation volumes and pressure changes at a critical cavitation rate of 0.1.

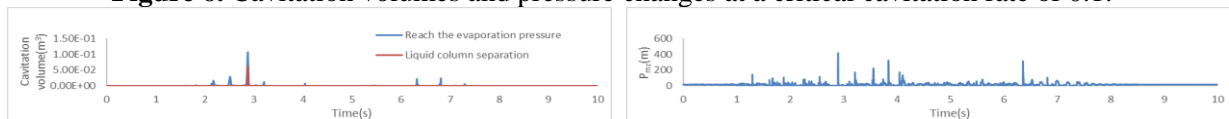


**Figure 7.** Cavity volumes and pressure changes at a critical cavitation rate of 0.15.

### 3.2. Analysis of sensitivity to frequency and amplitude of pulsating pressure

According to the calculation results in Section 3.2, continuous negative pressure of low frequency and the amplitude of negative pressure are important influencing factors that determine the occurrence of water column separation. On the basis of the previous section, this study examined the effects of frequency and amplitude of simple jagged pulsating pressure on the formation and development of cavity and the appearance of water column separation in this section.

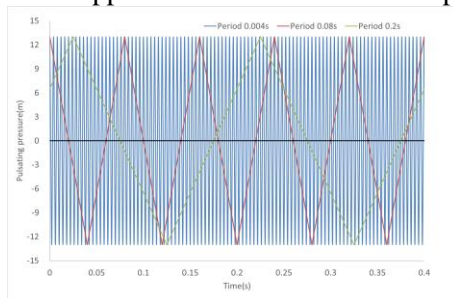


**Figure 8.** Pulsating pressure waves with different periods.

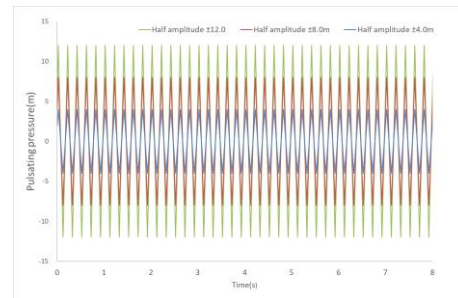


**Figure 9.** Pulsating pressure waves with different amplitudes.

(1) After the jagged pulsating pressures with an identical half-amplitude of  $\pm 13.0\text{m}$  and varying periods of 0.004s, 0.08s and 0.02s were applied on the 0-0 Section (as shown in Figure 8), the sensitivity to frequency was analyzed. It was found that the pulsating pressure dropped progressively according to the square root of the reciprocal of the distance from the 0-0 Section along the pipe axis. By setting the critical cavitation rate as 0.05, 0.10 and 0.15, the changes of the volume of cavitation volumes in the segment between the 0-0 Section and the 1-1 Section when the overall pressure reaches the evaporation pressure and liquid column separation occurs and the pressure on the 0-0 Section were analyzed, as the results shown in Figure 10~Figure 12.

(2) After the jagged pulsating pressures with an identical period of 0.2 s and varying half-amplitudes

of  $\pm 4.0\text{m}$ ,  $\pm 8.0\text{m}$  and  $\pm 12.0\text{m}$  were applied on the 0-0 Section (as shown in Figure 9), the sensitivity to amplitude was analyzed. It was also found that the pulsating pressure dropped steadily according to the square root of the reciprocal of the distance from the 0-0 Section along the pipe axis. By setting the critical cavitation rate as 0.05, 0.10 and 0.15, the changes of the volume of cavitation volumes in the segment between the 0-0 Section and the 1-1 Section when the overall pressure reaches the evaporation pressure and liquid column separation occurs and the pressure on the 0-0 Section were analyzed, as the results shown in Figure 13~Figure 15.

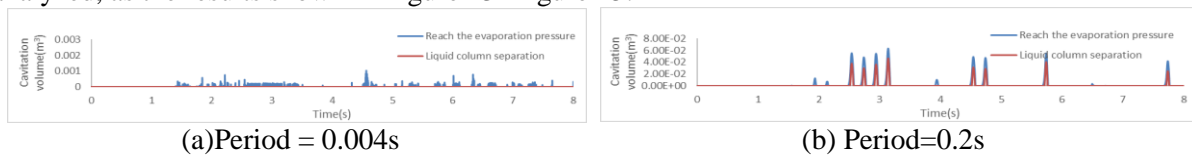


Figure 10. Cavitation volumes and pressure changes at a critical cavitation rate of 0.05.

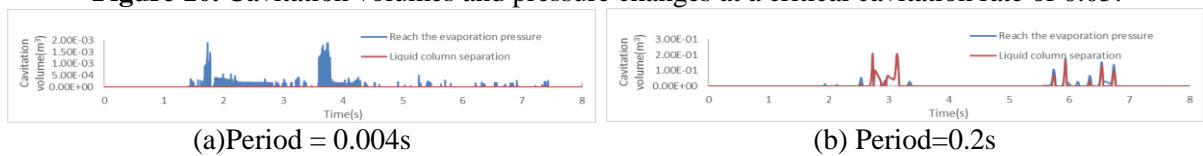


Figure 11. Cavitation volumes and pressure changes at a critical cavitation rate of 0.1.

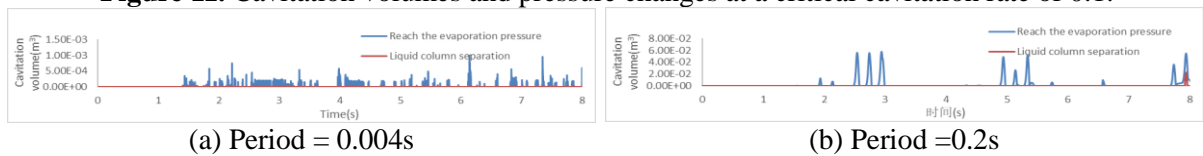


Figure 12. Cavitation volumes and pressure changes at a critical cavitation rate of 0.15.

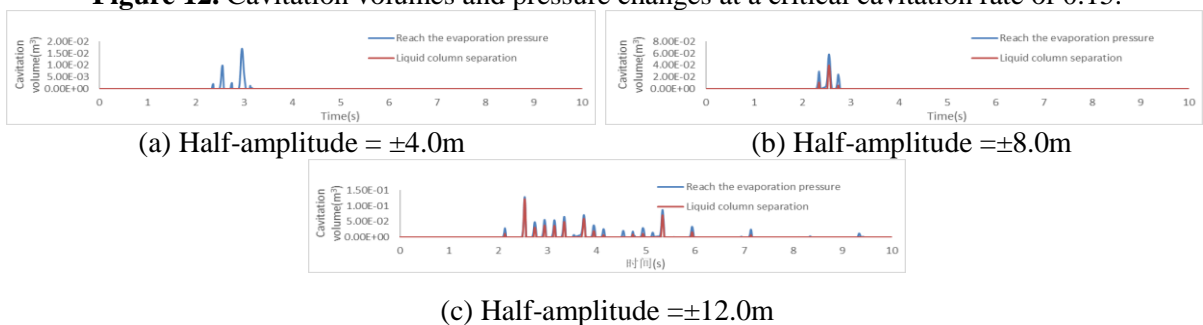


Figure 13. Cavitation volumes and pressure changes at a critical cavitation rate of 0.05.

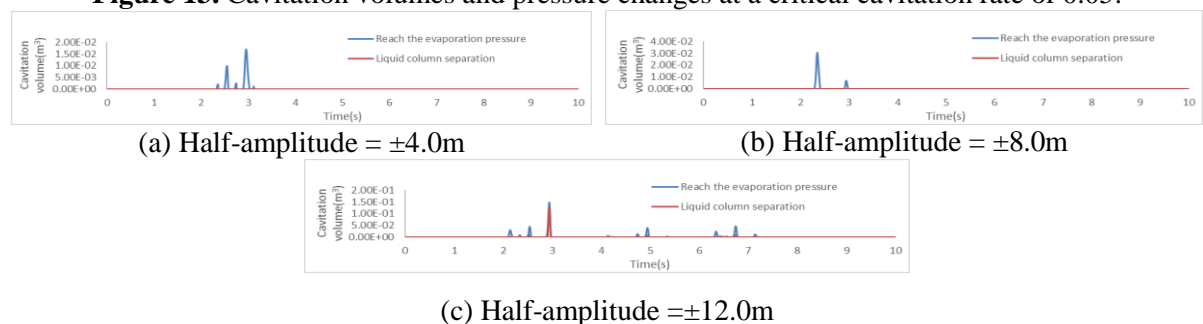


Figure 14. Cavitation volumes and pressure changes at a critical cavitation rate of 0.1.

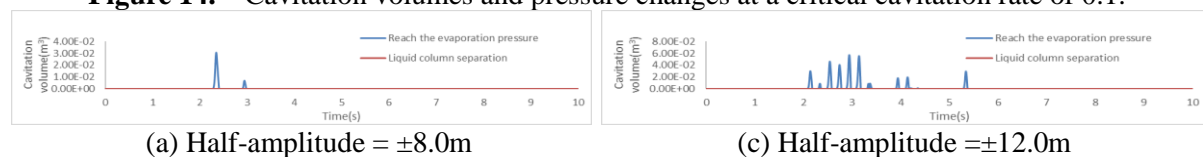


Figure 15. Cavitation volumes and pressure changes at a critical cavitation rate of 0.15.

According to above calculated results, the following conclusions can be drawn.

- (1) After the application of high-frequency pulsating pressure at a period of 0.004 s, the vaporous

cavitations in the pipe segment from the 0-0 Section to the 1-1 Section appeared and collapsed at high frequency. The formed vaporous cavitations were quite small in volume. No water column separation appeared whether the critical cavitation rate was set as 0.05, 0.10 or 0.15. As the pulsating pressure frequency dropped, both maintenance time and volume of vaporous cavitations in the pipe segment increased. At a period of 0.2 s, several water column separations occurred whether the critical cavitation rate was set as 0.05, 0.10 and 0.15.

(2) When the pulsating pressure with a half-amplitude of  $\pm 4.0\text{m}$  was applied, the pressure in the segment from the 0-0 section and the 1-1 section reached the evaporation pressure and vaporous cavitations appeared. No water column separation appeared whether the critical cavitation rate was set as 0.05, 0.10 or 0.15. After the application of the pulsating pressure with a half-amplitude of  $\pm 8.0\text{m}$ , the pressure in the pipe segment reached the evaporation pressure and vaporous cavitations were generated at a critical cavitation rate of 0.05, accompanied with water column separation. No water column separation appeared at a critical cavitation rate of 0.1 or 0.15. After the application of the pulsating pressure with a half-amplitude of  $\pm 12.0\text{m}$ , water column separation appeared; however, no water column separation appeared at a critical cavitation rate of 0.15.

#### 4. Conclusions

(1) After the application of high-frequency pulsating pressure at a period of 0.004 s, the vaporous cavitations in the pipe segment from the 0-0 Section to the 1-1 Section appeared and collapsed at high frequency. The formed vaporous cavitations were small in volume. No water column separation appeared in the segment at a critical cavitation rate of 0.05, 0.10 and 0.15. As the frequency of pulsating pressure dropped, both maintenance time and volume of the vaporous cavitations in the segment increased. Several water column separations appeared after the application of pulsating force at a period of 0.2 s whether the critical cavitation rate was set as 0.05, 0.10 or 0.15.

(2) After the application of the pulsating pressure with a half-amplitude of  $\pm 4.0\text{m}$ , the pressure in the segment between the 0-0 Section and the 1-1 Section reached the evaporation pressure and vaporous cavitations were generated. No water column separation can be observed in the segment at a critical cavitation rate of 0.05, 0.10 and 0.15. When the pulsating pressure with a half-amplitude of  $\pm 8.0\text{m}$  was applied, the pressure in the segment reached the evaporation pressure and vaporous cavitation were generated at a critical cavitation rate of 0.05, and meanwhile, water column separation appeared. At a critical cavitation rate of 0.1 and 0.15, no water column separation appeared. After the application of the pulsating pressure with a half-amplitude of  $\pm 12.0\text{m}$ , water column separation appeared; however, no water column separation occurred at a critical cavitation rate of 0.15.

#### Acknowledgment

This work was supported by the National Natural Science Foundation of China (NSFC) (No.51379158). This work was also supported by the POSTDOC workstation of Zhongnan Engineering Corporation Limited.

#### References

- [ 1 ] Kranenburg C 1972 The effects of free gas on cavitation in pipe-lines *Proceedings of the 1st International Conference on Pressure Surges, British Hydromechanics Research Association* 41-52
- [ 2 ] Wylie E B and Streeter V L 1993 *Fluid Transients in System* (Englewood Cliffs: Prentice-Hall)
- [ 3 ] Bergant A Simpson A R and Tijsseling A S 2006 Water hammer with column separation: A historical review *Journal of Fluids and Structures* **22**(2) 135-171
- [ 4 ] Yang J D 1984 *Study on the Transient Process of Gas-Liquid Two-Phase Flow* (Wuhan: Wuhan Institute of Water Conservancy and Electric Power)
- [ 5 ] Wu Y Q and Chen J Z 1997 *Hydraulic Transient Process of Hydropower Station* (Beijing: China Water Conservancy and Hydropower Press)